GRANT: NAG1-1626

IMPLEMENTATION OF FREE-FORMULATION-BASED FLAT SHELL ELEMENTS INTO NASA COMET CODE AND DEVELOPMENT OF NONLINEAR SHALLOW SHELL ELEMENT

NASA LANGLEY RESEARCH CENTER

PRINCIPAL INVESTIGATOR:

ERDOGAN MADENCI
AEROSPACE AND MECHANICAL ENGINEERING
UNIVERSITY OF ARIZONA
TUCSON, AZ 85721

NONLINEAR ELASTIC DEFORMATIONS OF MODERATELY THICK LAMINATED SHELLS SUBJECTED TO LARGE AND RAPID RIGID-BODY MOTION

A. Barut, E. Madenci

Department of Aerospace and Mechanical Engineering
The University of Arizona
Tucson, AZ 85721

and

A. Tessler

NASA Langley Research Center
Hampton, VA 23665

Abstract

This study presents a transient nonlinear finite element analysis within the realm of a multi-body dynamics formulation for determining the dynamic response of a moderately thick laminated shell undergoing a rapid and large rotational motion and nonlinear elastic deformations. Nonlinear strain measure and rotation, as well as the transverse shear deformation, are explicitly included in the formulation in order to capture the proper motion-induced stiffness of the laminate. The equations of motion are derived from the virtual work principle. The analysis utilizes a shear deformable shallow shell element along with the co-rotational form of the updated Lagrangian formulation. The shallow shell element formulation is based on the Reissner-Mindlin and Marguerre theory.

Introduction

Thick laminated composites such as helicopter blades can experience large elastic displacement and rotations due to rapid and large rotational motions. Any attempt to design composite helicopter blades must include the effect of motion-induced stiffness in both the longitudinal and chordwise directions. The stress analysis capability must account for the interaction of the nonlinear elastic deformations with the overall dynamic motion.

Review of previous studies relevant to helicopter blade design reveals that the majority of the analyses are limited to beam-type approximations, disregarding the chordwise deformations. In order to eliminate this shortcoming, Bhumbla and Kosmatka [1], Bauchau and Chiang [2], and Kosmatka [3] employed shear deformable shell elements within analyses restricted to rotating laminates under constant angular velocity. Their formulations exclude the effect of spin-up time, during which the angular velocity is not constant. Furthermore, the influence of the coupling between the rigid-body motion and the flexible deformation is not reflected in the construction of the mass matrix in any of these models. The inertial loads are treated as known external forces. Within multibody dynamics formalism, the mass matrix should include the coupling between the rigid-body motion, inertial forces, and the elastic deformations so that the inertial loads can be determined as part of the solution. Changes in inertial loads due to spin-up or external loads become important, especially in aeroelastic tailoring of the composite blades.

In order to account for this discrepancy, Bauchau and Kang [4] considered a multibody dynamics formulation coupled with elastic deformations. Their analysis, however, employs only beam-type finite elements. Extensive reviews of relevant multibody dynamics formulations coupled with elastic deformations can be found in Boutaghou et al. [5] and Tsang [6].

Although the response of an elastic beam subjected to a sudden slew rate coupled with large elastic deformations has been investigated extensively, there are no analyses

regarding the dynamic response of an elastic shell undergoing large overall motion accompanied by large elastic displacements and rotations. Banarjee and Kane [7], Banerjee and Dickens [8], Chang and Shabana [9-10], Boutaghou et al. [5], and Tsang [6] included the interaction of large overall motion and *small* strain elastic deformations. The complexity of the problem arising from the interaction of large rigid-body translational and rotational motions and large displacements and rotations renders the analytical and numerical predictions very difficult.

All of these previous analyses are limited to isotropic plates and suffer from loss of additional motion-induced stiffness due to large elastic displacements (membrane and bending) and rotations. Also, they require that the rigid-body motion be known *a priori*. The coupling between bending and stretching and bending and twisting in anisotropic composite plates and the presence of initial curvature further complicate the problem.

The present analysis is aimed at capturing the motion-induced membrane and bending stiffness variations by explicitly including the nonlinear strain measure and rotations and the transverse shear deformations. It is to be noted that none of the available finite element analyses, including commercial programs, have the capability to solve this problem within the realm of multibody dynamics formalism. The transverse shear deformation, which is essential for accurate failure prediction of thick composite laminates, is included by extending Tessler's [11] shallow shell element into the nonlinear range and its implementation into the transient finite element formulation within the framework of multibody dynamics formalism.

Equations of Motion

The kinematic description of a point P in a three-noded shallow shell element between time t and t + Δt is illustrated in Fig. 1. The equations of motion are derived based on the concept of virtual displacements in conjunction with the co-rotational form of the updated Lagrangian description of motion. The formulation utilizes the inertial,

body-fixed, and element Cartesian coordinates as (x, y, z), (x', y', z'), and (x'', y'', z''), respectively. The configuration at time t + Δt represents the unknown current equilibrium configuration. The last known equilibrium configuration is at time t, and it is referred to as the updated configuration. In the updated Lagrangian form of the co-rotational approach, the current configuration utilizes the projection of the deformed element surface onto the x''-y'' plane of the element coordinate system in the updated configuration as a reference configuration. The angular velocity, $\Omega(t)$, of the shell arising from either a prescribed slew rate or external forces results in the rigid-body motion of the element coordinate system as the deformation proceeds.

Matrices Z and T are utilized in transforming a vector from the element coordinate system to the body-fixed frame and from the body-fixed frame to the inertial frame, respectively. A vector with a single prime or a double prime is defined with respect to base vectors of the body-fixed or element coordinate system, respectively.

In the absence of body forces, the virtual work done at time t + Δt in the kth element due to inertial, internal, and external forces is expressed as

$$\int_{{}^tV} \rho \, \delta \, {}^{t+\Delta t}\mathbf{R}^T \, {}^{t+\Delta t}\ddot{\mathbf{R}} \, d^tV + \int_{{}^tV} \delta \, {}_t\mathbf{E}^T \, {}^{t+\Delta t}_t\mathbf{S} \, d^tV = \delta \mathcal{W} \tag{1}$$

In this expression, the left subscript indicates the configuration by which the quantity is measured. The left superscript refers to the configuration of the body at a specific time. The volume of the kth facet shell element containing the point P at time t is denoted by ${}^tV$. Differentiation with respect to time is denoted by $\dot{(\cdot)}$ superscribed above the variable, and its virtual value by δ.

The position of point P at time t + Δt is described by the vector ${}^{t+\Delta t}\mathbf{R}$ in reference to the origin of the inertial coordinate system, (x, y z). The components of the incremental Green strain tensor and the Piola-Kirchhoff stress tensor associated with the kth element are contained in vectors ${}_t\mathbf{E}$ and ${}^{t+\Delta t}_t\mathbf{S}$, respectively. The virtual work for the kth element due to nodal forces and moments at time t + Δt is denoted by $\delta \mathcal{W}$. The constant mass density of the material is denoted by ρ.

Virtual Work by Inertial Forces. Based on the kinematics of motion as illustrated in Fig. 1, the position of point P in the kth element at time t + Δt is expressed as

$$^{t+\Delta t}\mathbf{R} = {}^{t+\Delta t}\mathbf{R}_0 + {}^{t+\Delta t}\mathbf{r} \tag{2}$$

where $^{t+\Delta t}\mathbf{R}_0$ describes the rigid-body motion of the shell by the position of the origin of the body-fixed frame (x', y', z') at time t + Δt. Relative to this body-fixed frame, the point P undergoes rigid- and flexible-body motions from the previously known configuration to the current (unknown) configuration. Between time t and t + Δt, the rigid-body motion and elastic deformation of point P are specified by $^{t}\mathbf{r}$ and $^{t+\Delta t}\mathbf{u}$, respectively. In reference to the body-fixed frame, the position of point P at time t + Δt is given by $^{t+\Delta t}\mathbf{r}$. (In the remaining expressions, the left superscript is dropped for simplicity unless it is different from t + Δt.) Applying the variational operator to Eq. (2), with the use of the transformation

$$\mathbf{r} = \mathbf{T}\mathbf{r}', \qquad \text{with } \mathbf{r}' = {}^{t}\mathbf{r}' + \mathbf{u}' \tag{3}$$

and the variation of T given by

$$\delta\mathbf{T} = \delta\tilde{\boldsymbol{\omega}}\,\mathbf{T} \tag{4}$$

puts Eq. (2) in the following form:

$$\delta\mathbf{R} = \delta\mathbf{R}_0 - \mathbf{T}\,\tilde{\mathbf{r}}'\,\mathbf{T}^{\mathsf{T}}\delta\boldsymbol{\omega} + \mathbf{T}\delta\mathbf{u}' \tag{5}$$

where $\delta\boldsymbol{\omega}$ is the virtual rigid-body rotation vector. Hereafter, "~" indicates a skew-symmetric matrix and $\delta\tilde{\boldsymbol{\omega}}$ is a skew-symmetric matrix with virtual rotations of the body-fixed frame.

The acceleration at point P is given by

$$\ddot{\mathbf{R}} = \ddot{\mathbf{R}}_0 - \mathbf{T}\,\tilde{\mathbf{r}}'\,\mathbf{T}^{\mathsf{T}}\dot{\boldsymbol{\Omega}} + \mathbf{T}\ddot{\mathbf{u}}' + 2\tilde{\boldsymbol{\Omega}}\mathbf{T}\dot{\mathbf{u}}' + \tilde{\boldsymbol{\Omega}}\tilde{\boldsymbol{\Omega}}\mathbf{T}\mathbf{r}' \tag{6}$$

Relative to the body-fixed frame, the incremental displacement vector, $\mathbf{u}'$, is expressed in terms of the incremental total nodal vector, $\mathbf{v}'$, as

$$\mathbf{u}' = \mathbf{N}'_m \mathbf{v}' \tag{7}$$

based on the finite element displacement approximation with the interpolation matrix, $\mathbf{N}'_m$. The total nodal vector consists of the incremental elastic displacement, $\mathbf{u}'_{0i}$, and rotation, $\boldsymbol{\theta}'_{0i}$, at each node of the kth shallow shell element shown in Fig. 2 and is defined as

$$\mathbf{v}'^T = \{\mathbf{v}'^T_1 \quad \mathbf{v}'^T_2 \quad \mathbf{v}'^T_3\} \tag{8}$$

in which $\mathbf{v}'^T_i = \{\mathbf{u}'^T_{0i} \quad \boldsymbol{\theta}'^T_{0i}\}$. As suggested by Christensen and Lee [12], the negligible time variation of the interpolation matrix, $\mathbf{N}'_m$, leads to

$$\dot{\mathbf{u}}' = \mathbf{N}'_m \dot{\mathbf{v}}' \quad \text{and} \quad \ddot{\mathbf{u}} = \mathbf{N}'_m \ddot{\mathbf{v}}' \tag{9}$$

Utilizing the transformation matrix, Z, associated with the kth element, the incremental displacement vector, $\mathbf{u}'$, is expressed as

$$\mathbf{u}' = \mathbf{Z}\mathbf{u}'' \tag{10}$$

The transformation between the incremental total nodal vectors defined relative to the body-fixed and element frames is achieved by

$$\mathbf{v}' = \mathbf{Z}^* \mathbf{v}'' \tag{11}$$

The transformation matrix, $\mathbf{Z}^*$, is defined as

$$\mathbf{Z}^* = \begin{bmatrix} \mathbf{Z} & \mathbf{0} \\ \mathbf{0} & \mathbf{Z}_\theta \end{bmatrix} \delta_{ij} \qquad i,j = 1,3 \tag{12}$$

in which δ_{ij} is the Kronecker delta and $\mathbf{Z}_\theta$ is the transformation matrix relating the rotations between the element coordinate system and the body-fixed frame as

$$\theta'_0 = Z_\theta \theta''_0 \tag{13}$$

Using the interpolation matrix, $\mathbf{N}''_m$, the incremental displacement vector, $\mathbf{u}''$, is approximated in terms of the incremental total nodal vector, $\mathbf{v}''$, as

$$\mathbf{u}'' = \mathbf{N}''_m \mathbf{v}'' \tag{14}$$

Based on the Reissner-Mindlin plate theory, the incremental displacement vector for a flat laminate can be expressed as

$$\mathbf{u}'' = \begin{Bmatrix} u(x'', y'', z'') \\ v(x'', y'', z'') \\ w(x'', y'', z'') \end{Bmatrix} = \begin{Bmatrix} u_0(x'', y'') \\ v_0(x'', y'') \\ w_0(x'', y'') \end{Bmatrix} + z'' \begin{Bmatrix} \theta_{y''}(x'', y'') \\ \theta_{x''}(x'', y'') \\ 0 \end{Bmatrix} \tag{15a}$$

or

$$\mathbf{u}'' = \mathbf{u}''_0 + z''\theta''_0 \tag{15b}$$

in which u_0, v_0, and w_0 represent mid-surface displacements. The in-plane displacement components in the x'' and y'' directions are denoted by u and v, respectively. The out-of-plane deflection is represented by w. The incremental displacement and rotation vectors associated with the mid-surface, $\mathbf{u}''_0$ and θ''_0, are approximated in terms of the nodal unknown displacements as

$$\mathbf{u}''_0 = \mathbf{N}_{mu}\mathbf{v}'' \quad \text{and} \quad \theta''_0 = \mathbf{N}_{m\theta}\mathbf{v}'' \tag{16}$$

where $\mathbf{v}''$ is the incremental total nodal vector and $\mathbf{N}_{mu}$ and $\mathbf{N}_{m\theta}$ are the interpolation matrices for translational and rotational displacement fields. Substituting for the mid-surface displacement and rotation vectors, $\mathbf{u}''_0$ and θ''_0, in Eq. (15) results in

$$\mathbf{u}'' = (\mathbf{N}_{mu} + z''\mathbf{N}_{m\theta})\mathbf{v}'' \tag{17}$$

Thus, the explicit form of the interpolation matrix, $\mathbf{N}''_m$, in Eq. (14) can be established as

$$\mathbf{N}''_m = \mathbf{N}_{mu} + z''\mathbf{N}_{m\theta} \tag{18}$$

Substituting from Eq. (14) into (10) in conjunction with Eq. (11) results in

$$\mathbf{u}' = \mathbf{Z}\mathbf{N}''_m\mathbf{Z}^{*T}\mathbf{v}' \tag{19}$$

Comparison of Eqs. (19) and (7) provides the expression for $\mathbf{N}'_m$ as

$$\mathbf{N}'_m = \mathbf{Z}\mathbf{N}''_m\mathbf{Z}^{*T} \tag{20}$$

After substituting from Eq. (9), along with Eq. (20), into Eqs. (5) and (6), the first integral, corresponding to the virtual work due to inertial forces in the kth element at time $t + \Delta t$, can be expressed in matrix form as

$$\int_{{}^tV} \rho\, \delta\mathbf{R}^T \ddot{\mathbf{R}}\, d{}^tV = \begin{Bmatrix} \delta\mathbf{R}_0 \\ \delta\boldsymbol{\omega} \\ \delta\mathbf{v}' \end{Bmatrix}^T \begin{bmatrix} \mathbf{M}_{RR} & \mathbf{M}_{R\omega} & \mathbf{M}_{Rv'} \\ & \mathbf{M}_{\omega\omega} & \mathbf{M}_{\omega v'} \\ \text{sym.} & & \mathbf{M}_{v'v'} \end{bmatrix} \begin{Bmatrix} \ddot{\mathbf{R}}_0 \\ \dot{\boldsymbol{\Omega}} \\ \ddot{\mathbf{v}}' \end{Bmatrix} + \begin{Bmatrix} \delta\mathbf{R}_0 \\ \delta\boldsymbol{\omega} \\ \delta\mathbf{v}' \end{Bmatrix}^T \begin{Bmatrix} \mathbf{f}_1 + \mathbf{f}_2 \\ \mathbf{g}_1 + \mathbf{g}_2 \\ \mathbf{h}_1 + \mathbf{h}_2 \end{Bmatrix} \tag{21}$$

in which

$$\mathbf{M}_{RR} = \rho\, {}^tV\, \mathbf{I}\,, \qquad \mathbf{M}_{R\omega} = -\rho\mathbf{T}\int_{{}^tV} \tilde{\mathbf{r}}'\, d{}^tV\, \mathbf{T}^T$$

$$\mathbf{M}_{Rv'} = \rho\mathbf{T}\mathbf{Z}\int_{{}^tV} \mathbf{N}''_m\, d{}^tV\, \mathbf{Z}^{*T}\,, \qquad \mathbf{M}_{\omega\omega} = -\rho\mathbf{T}\mathbf{Z}\int_{{}^tV} \tilde{\mathbf{r}}''\, \tilde{\mathbf{r}}''\, d{}^tV\, \mathbf{Z}^T\mathbf{T}^T$$

$$\mathbf{M}_{\omega v'} = \rho\mathbf{T}\mathbf{Z}\int_{{}^tV} \tilde{\mathbf{r}}''\mathbf{N}''_m\, d{}^tV\, \mathbf{Z}^{*T}\,, \qquad \mathbf{M}_{v'v'} = \rho\mathbf{Z}^*\int_{{}^tV} \mathbf{N}''^T_m\mathbf{N}''_m\, d{}^tV\, \mathbf{Z}^{*T}$$

$$\mathbf{f}_1 = 2\rho\mathbf{T}\mathbf{Z}\tilde{\boldsymbol{\Omega}}''\int_{{}^tV} \mathbf{N}''_m\, d{}^tV\, \dot{\mathbf{v}}''\,, \qquad \mathbf{f}_2 = \rho\mathbf{T}\tilde{\boldsymbol{\Omega}}'\tilde{\boldsymbol{\Omega}}'\int_{{}^tV} \mathbf{r}'\, d{}^tV$$

$$\mathbf{g}_1 = 2\rho\mathbf{T}\mathbf{Z}\int_{{}^tV} \tilde{\mathbf{r}}''\tilde{\boldsymbol{\Omega}}''\mathbf{N}''_m\, d{}^tV\, \dot{\mathbf{v}}''\,, \qquad \mathbf{g}_2 = \rho\mathbf{T}\mathbf{Z}\int_{{}^tV} \tilde{\mathbf{r}}''\tilde{\boldsymbol{\Omega}}''\tilde{\boldsymbol{\Omega}}''\mathbf{r}''\, d{}^tV$$

$$h_1 = 2\rho Z^* \int_{{}^tV} {N''_m}^T \tilde{\Omega}'' N''_m \, d^tV \, \dot{v}'', \qquad h_2 = \rho Z^* \int_{{}^tV} {N''_m}^T \tilde{\Omega}'' \tilde{\Omega}'' r'' \, d^tV$$

where the identity matrix is denoted by **I**.

Virtual work by internal stresses. The second integral, representing the virtual work by internal stresses, in Eq. (1) can be expressed for a laminated composite material in the form [13]

$$\sum_{k=1}^{K} \int_{{}^tA} \int_{h_{k-1}}^{h_k} \delta \, {}_tE_L^T \, \bar{Q}^{(k)} \, {}_tE_L \, dz \, d^ta + \sum_{k=1}^{K} \int_{{}^tA} \int_{h_{k-1}}^{h_k} \delta \, {}_tE_{NL}^T \, {}^t\sigma^{(k)} \, dz \, d^ta$$

$$+ \sum_{k=1}^{K} \int_{{}^tA} \int_{h_{k-1}}^{h_k} \delta \, {}_tE_L^T \, {}^t\sigma^{(k)} \, dz \, d^ta \tag{22}$$

where K denotes the number of layers in the laminate. The position of the layers in reference to the mid-surface is specified by h_k. The thickness of the kth layer is given by $t_k = h_k - h_{k-1}$. At time t, ${}^tA$ represents the projections of the surface area on the (x'', y'') plane. The stress and strain components are related through the relation $\sigma^{(k)} = \bar{Q}^{(k)} E_L$, in which $\bar{Q}^{(k)}$ is for the kth orthotropic lamina referenced to the arbitrary axes. Each layer is assumed to be homogeneous, elastic, and orthotropic with elastic moduli, E_L and E_T; shear modulus, G_{LT}; and Poisson's ratio, ν_{LT}. The subscripts L and T specify the longitudinal and transverse directions relative to the fibers in the layer with thickness t.

The linear and nonlinear components of the Green's strain tensor in vector form are expressed as

$$\left.\begin{aligned} E_L &= \begin{Bmatrix} u_{0,x''} \\ v_{0,y''} \\ u_{0,y''}+v_{0,x''} \end{Bmatrix} + z'' \begin{Bmatrix} \theta_{y'',x''} \\ \theta_{x'',y''} \\ 0 \end{Bmatrix} - \begin{Bmatrix} h_{0,x''}\theta_{y''} \\ h_{0,y''}\theta_{x''} \\ h_{0,x''}\theta_{x''} + h_{0,y''}\theta_{y''} \end{Bmatrix} \\ E_{NL} &= \frac{1}{2} \begin{Bmatrix} u_{0,x''}^2 + v_{0,x''}^2 + w_{0,x''}^2 \\ u_{0,y''}^2 + v_{0,y''}^2 + w_{0,y''}^2 \\ 2(u_{0,x''}u_{0,y''} + v_{0,x''}v_{0,y''} + w_{0,x''}w_{0,y''}) \end{Bmatrix} \end{aligned}\right\} \quad (23)$$

where $h_0(x'', y'')$ describes the surface of the shallow shell. As given by Tessler [11], the linear component of the Green strain tensor is based on the Reissner-Mindlin definition combined with the Marguerre shallow shell theory. The nonlinear strain vector, E_{NL}, is an approximation to its complete form.

Substituting for the strain components and performing integration along the transverse direction in Eq. (22) lead to

$$\int_{t_A} \delta\, {}_t e_L^T\, C\, {}_t e_L\, d^t a + \int_{t_A} \delta\, {}_t E_{NL}^T\, {}^t s_m\, d^t a + \int_{t_A} \delta\, {}_t e_L^T\, {}^t s\, d^t a \quad (24)$$

in which C is composed of the extensional, coupling, bending, and transverse stiffness matrices, A, B, D, and G

$$C = \begin{bmatrix} A & B & 0 \\ B & D & 0 \\ 0 & 0 & G \end{bmatrix}$$

the vector ${}^t s$, which contains the in-plane resultant forces, ${}^t s_m$, moments, ${}^t s_b$, and shear resultant forces, ${}^t s_q$, is in the form

$${}^t s^T = \{{}^t s_m \quad {}^t s_b \quad {}^t s_q\} \quad (25)$$

The vector ${}_t\mathbf{e}_L$ is composed of incremental mid-plane strain, curvature, and transverse shear components,

$$
\begin{aligned}
{}_t\mathbf{e}_L = \{ & u_{0,x''} - h_{0,x''}\theta_{y''},\ v_{0,y''} - h_{0,y''}\theta_{x''},\ u_{0,y''} + v_{0,x''} - h_{0,x''}\theta_{x''} \\
& - h_{0,y''}\theta_{y''},\ \theta_{y'',x''},\ \theta_{x'',y''},\ \theta_{x'',x''} + \theta_{y'',y''},\ w_{0,x''} + \theta_{y''},\ w_{0,y''} + \theta_{x''}\}
\end{aligned} \tag{26}
$$

The incremental in-plane mid-plane displacement components are approximated by cubic interpolation functions, $\mathcal{N}_{sk}$ and $\mathcal{N}_{sc}$, as in Tessler [11],

$$
\begin{Bmatrix} u_0 \\ v_0 \end{Bmatrix} = \sum_{k=1}^{3} \mathcal{N}_{sk} \begin{Bmatrix} u_{0k} \\ v_{0k} \end{Bmatrix} + \sum_{k=4}^{9} \mathcal{N}_{sk} \begin{Bmatrix} u_{0k} \\ v_{0k} \end{Bmatrix} + \mathcal{N}_{sc} u_{0c} \tag{27}
$$

where u_{0k} and v_{0k} are the in-plane displacements specified at the nodes. The displacements corresponding to the corner nodes are specified by u_{0k}, v_{0k} with k = 1, 2, 3. The remaining u_{0k} and v_{0k} represent the intra-edge displacements. The displacements at the center of the element are given by u_{0c}. The mid-plane transverse displacement field is approximated by a quadratic interpolation function, $\mathcal{M}_{sk}$, as

$$
w_0 = \sum_{k=1}^{6} \mathcal{M}_{sk} w_{0k} \tag{28}
$$

where w_{0k} correspond to the corner and mid-edge nodes.

The mid-plane out-of-plane rotational components are approximated by linear interpolation functions, ξ_k, as

$$
\begin{Bmatrix} \theta_{x''} \\ \theta_{y''} \end{Bmatrix} = \sum_{k=1}^{3} \xi_k \begin{Bmatrix} \theta_{x''k} \\ \theta_{y''k} \end{Bmatrix} \tag{29}
$$

where $\theta_{x''k}$ and $\theta_{y''k}$ are nodal rotations at the corner nodes.

In matrix notation, Eqs. (27)-(29) can be rewritten as

$$
\mathbf{u}''_0 = \mathbf{N}_{su}\mathbf{v}'' + \overset{+}{\mathbf{N}}_{su}\overset{+}{\mathbf{v}}'' + \mathbf{N}_{sc}\mathbf{v}''_c \tag{30}
$$

$$\theta''_0 = \mathbf{N}_{s\theta}\,\mathbf{v}'' \tag{31}$$

where

$$\mathbf{u}''^{T}_0 = \{w_0,\ v_0,\ w_0\} \quad \text{and} \quad \theta''^{T}_0 = \{\theta_{x''},\ \theta_{y''},\ 0\}$$

$$\mathbf{v}''^{T} = \{w_{01},\ v_{01},\ w_{01},\ \theta_{x''1},\ \theta_{y''1},\ \theta_{z''1},\ \ldots,\ w_{03},\ v_{03},\ w_{03},\ \theta_{x''3},\ \theta_{y''3},\ \theta_{z''3}\}$$

$$\overset{+}{\mathbf{v}}''^{T} = \{w_{04},\ \ldots,\ w_{09},\ v_{04},\ \ldots,\ v_{09},\ w_{04},\ w_{05},\ w_{06}\}$$

$$\mathbf{v}''^{T}_c = \{w_{0c},\ v_{0c}\}$$

The matrix of interpolation functions, $\mathbf{N}_{su}$, is dependent on $\mathcal{N}_{si}$ and $\mathcal{M}_{si}$ (i = 1, 2, 3). The shape function matrix, $\overset{+}{\mathbf{N}}_{su}$, involves $\mathcal{N}_{si}$ (i = 4, ..., 9) and $\mathcal{M}_{si}$ (i = 4, ..., 6). The matrix $\mathbf{N}_{sc}$ contains only $\mathcal{N}_{sc}$. The shape matrix, $\mathbf{N}_{s\theta}$, is composed of the area coordinates ξ_i (i = 1, 3). Although $\theta_{z''k}$ (k = 1, 2, 3) do not exist, they are included in the formulation because the transformation to body-fixed coordinates leads to non-zero rotations in all axes.

The intra-edge displacements included in $\overset{+}{\mathbf{v}}''$ are expressed in terms of corner displacements, $\mathbf{v}''$, through an appropriate transformation

$$\overset{+}{\mathbf{v}}'' = \mathbf{L}\,\mathbf{v}'' \tag{32}$$

The transformation matrix, L, is obtained by imposing constant strain conditions along the three edges of the element. The explicit form of these constraints and the detailed form of L (in partitioned form) are given by Tessler [11].

Substituting from Eq. (4) into Eq. (30) and combining the resulting equation with Eq. (31) lead to

$$\begin{Bmatrix} \mathbf{u}''_0 \\ \theta''_0 \end{Bmatrix} = \begin{bmatrix} \mathbf{N}^{*}_{su} & \mathbf{N}_{sc} \\ \mathbf{N}_{s\theta} & 0 \end{bmatrix} \begin{Bmatrix} \mathbf{v}'' \\ \mathbf{v}''_c \end{Bmatrix} \tag{33}$$

where $\mathbf{N}^{*}_{su} = \mathbf{N}_{su} + \overset{+}{\mathbf{N}}_{su}\mathbf{L}$. This relationship can be taken as the basis in formulating the

strain-displacement transformation matrix, $\mathcal{B}_s$, in the form

$$\mathcal{B}_s = [\mathcal{B}_{su}, \mathcal{B}_{s\theta}] \tag{34}$$

where $\mathcal{B}_{su}$ and $\mathcal{B}_{s\theta}$ are defined such that the resultant strain vector, ${}_te_L$, given by Eq. (26) can be obtained from

$${}_te_L = [\mathcal{B}_{su}, \mathcal{B}_{s\theta}] \begin{Bmatrix} u''_0 \\ \theta''_0 \end{Bmatrix} \tag{35}$$

This form of vector ${}_te_L$ allows the first integral in Eq. (24) to be rewritten as

$$\int_{t_A} \delta\, {}_te_L^T\, C\, {}_te_L\, d\, {}^ta = \begin{Bmatrix} \delta v'' \\ \delta v''_c \end{Bmatrix}^T \begin{bmatrix} k_{L11} & k_{L12} \\ k_{L12}^T & k_{L22} \end{bmatrix} \begin{Bmatrix} v'' \\ v''_c \end{Bmatrix} \tag{36}$$

with

$$k_{L11} = \int_{t_A} (N_{su}^{\cdot T} \mathcal{B}_{su}^T C\, \mathcal{B}_{su} N_{su}^{\cdot} + N_{su}^{\cdot T} \mathcal{B}_{su}^T C\, \mathcal{B}_{s\theta} N_{s\theta} + N_{s\theta}^T \mathcal{B}_{s\theta}^T C\, \mathcal{B}_{su} N_{su}^{\cdot} + N_{s\theta}^T \mathcal{B}_{s\theta}^T C\, \mathcal{B}_{s\theta} N_{s\theta})\, d\, {}^ta$$

$$k_{L12} = \int_{t_A} (N_{su}^{\cdot T} \mathcal{B}_{su}^T C\, \mathcal{B}_{su} N_{sc} + N_{s\theta}^T \mathcal{B}_{s\theta}^T C\, \mathcal{B}_{su} N_{sc})\, d\, {}^ta$$

and

$$k_{L22} = \int_{t_A} N_{sc}^T \mathcal{B}_{su}^T C\, \mathcal{B}_{su} N_{sc}\, d\, {}^ta$$

Assuming external or internal loads are not applied at the center node of the element, the stiffness matrix, k_L, can be condensed statically to a smaller sized matrix, $k_L^{\cdot}$,

$$k_L^{\cdot} = k_{L11} - k_{L12} k_{L22}^{-1} k_{L12}^T \tag{37}$$

where $k_L^{\cdot}$ represents the condensed stiffness matrix. It consists of six degrees of freedom, including the θ_z artificial degree of freedom at each corner node.

The second integral in Eq. (24) can be rewritten in terms of the total nodal vector as

$$\int_{t_A} \delta\, {}_tE_{NL}^T\, {}^ts_m\, d^ta = \delta\, \mathbf{v}''^T\, \mathbf{k}_g\, \mathbf{v}'' \tag{38}$$

where the geometric stiffness matrix, $\mathbf{k}_g$, is defined by

$$\mathbf{k}_g = \int_{t_A} \mathbf{N}_{mu}^T\, \mathcal{B}^T\, {}^tS_m\, \mathcal{B}\, \mathbf{N}_{mu}\, d^ta \tag{39}$$

in which the matrix differential operator $\mathcal{B}$ and ${}^tS_m$ are explicitly given by Madenci and Barut [13]. The tangential stiffness matrix, $\mathbf{k}_T$, is defined by

$$\mathbf{k}_T = \mathbf{k}_L^{\cdot} + \mathbf{k}_g \tag{40}$$

By substituting from Eqs. (25) and (35), the third integral in Eq. (24) can be rewritten in the form

$$\int_{t_A} \delta\, {}_te_L^T\, {}^ts\, d^ta = \delta\, \mathbf{v}''^T\, \mathbf{k}_L^{\cdot}\, \mathbf{v}''' \tag{41}$$

The vector of nodal displacements, $\mathbf{v}'''$, corresponds to local deformations between the initial and the updated configurations of the elements. It is determined by subtracting the rigid-body motion from the total displacements. The deformational out-of-plane nodal rotations are determined by the methods provided by Rankin and Brogan [14].

With the use of Eqs. (36), (38), and (41), in conjunction with Eq. (11), the second integral, representing the virtual work by internal stresses in the kth element, is expressed in matrix form as

$$\int_{{}^tV} \delta_t E^T \, {}^{t+\Delta t}_{t}S \, d\,{}^tV = \begin{Bmatrix} \delta R_0 \\ \delta\omega \\ \delta v' \end{Bmatrix}^T \begin{bmatrix} 0 & 0 & 0 \\ 0 & 0 & 0 \\ 0 & 0 & k'_T \end{bmatrix} \begin{Bmatrix} R_0 \\ \omega \\ v' \end{Bmatrix} + \begin{Bmatrix} \delta R_0 \\ \delta\omega \\ \delta v' \end{Bmatrix}^T \begin{Bmatrix} 0 \\ 0 \\ k'_L v'' \end{Bmatrix} \quad (42)$$

where

$$k'_T = Z^*(k^*_L + k_g)Z^{*T} \quad \text{and} \quad k'_L = Z^* k_L Z^{*T}$$

Virtual work by external forces. The virtual work due to nodal forces and moments at the ith node of the kth element is expressed as

$$\delta\mathcal{W}_i = \delta R_i^T F_i + (\delta\omega^T + \delta\theta_i^T)M_i \quad (43)$$

in which F_i and M_i are the nodal force and moment vectors, respectively, at the ith node. The position of the ith node in the kth element with respect to the origin of the inertial frame is specified by R_i. The virtual rigid-body rotation of this element is represented by $\delta\omega$, and its elastic rotation at the ith node by a vector, $\delta\theta_i$. Substituting for δR_i from Eq. (5) into Eq. (43) and using the property of the transformation matrix, T, result in

$$\delta\mathcal{W}_i = \delta R_0^T F_i + \delta\omega^T T(\tilde{r}'_i F'_i + M'_i) + \delta u_i'^T F'_i + \delta\theta_i'^T M'_i \quad (44)$$

Adding the contribution of each node and utilizing the definition of $v_i'^T$ result in the following expression for virtual work due to external loads in the kth element:

$$\delta\mathcal{W} = \begin{Bmatrix} \delta R_0 \\ \delta\omega \\ \delta v' \end{Bmatrix}^T \begin{Bmatrix} \bar{F} \\ \bar{M} \\ P' \end{Bmatrix} \quad (45)$$

where

$$\bar{F} = \sum_{i=1}^{3} F_i \,, \qquad \bar{M} = T\sum_{i=1}^{3} (\tilde{r}'_i F'_i + M'_i)$$

and

$$P'^T = \{P'^T_1 \quad P'^T_2 \quad P'^T_3\}, \qquad \text{with} \qquad P'^T_i = \{F'^T_i \quad M'^T_i\}$$

Finite element equations of motion. Substituting Eqs. (21), (42), and (45) into the expression for virtual work (Eq. 1) and requiring the virtual quantities δR_0, $\delta\omega$, and $\delta v'$ to be arbitrary result in the coupled and highly nonlinear equations of motion between time t and t + Δt for the finite element:

$$\mathbf{M}(\mathbf{b})\ddot{\mathbf{b}} + \mathbf{f}^\sigma(\mathbf{b}) = \mathbf{f}(\mathbf{b}) \tag{46}$$

The solution vector, **b**, the mass matrix, **M**, and the vector, **f**, arising from external and gyroscopic forces are defined as

$$\mathbf{b} = \begin{Bmatrix} R_0 \\ \omega \\ v' \end{Bmatrix}; \quad \mathbf{M} = \begin{bmatrix} M_{RR} & M_{R\omega} & M_{Rv'} \\ & M_{\omega\omega} & M_{\omega v'} \\ \text{Sym.} & & M_{v'v'} \end{bmatrix}; \quad \mathbf{f} = \begin{Bmatrix} \bar{F} - f_1 - f_2 \\ \bar{M} - g_1 - g_2 \\ P' - h_1 - h_2 \end{Bmatrix}$$

The vector due to internal stresses, $\mathbf{f}^\sigma$, is given by

$$\mathbf{f}^\sigma = \mathbf{K}_T(\mathbf{b})\mathbf{b} + {}^t\mathbf{f}^\sigma \tag{47}$$

where

$$\mathbf{K}_T = \begin{bmatrix} 0 & 0 & 0 \\ 0 & 0 & 0 \\ 0 & 0 & k'_T \end{bmatrix} \quad \text{and} \quad {}^t\mathbf{f}^\sigma = \begin{Bmatrix} 0 \\ 0 \\ k'_L v''' \end{Bmatrix}$$

The vector ${}^t\mathbf{f}^\sigma$ is known from the previous increment between time t - Δt and t.

The equations of motion (46) for each element are assembled by usual techniques to form the global equations of motion. Their solution provides the motion of the origin of the body-fixed frame with respect to the inertial frame and the elastic deformations of the body with respect to the body-fixed frame.

Numerical Results

Solution of the nonlinear global equations of motion is achieved by means of the Newton-Raphson method in conjunction with the trapezoidal time integration scheme. The construction of the solution vector **b** at time t + Δt involves iterations that begin with the known solution vector $^t\mathbf{b}$ at time t. The ith iteration of the solution vector $\mathbf{b}_i$ is decomposed as

$$\mathbf{b}_i = \mathbf{b}_{i-1} + \Delta\mathbf{b} \tag{48}$$

In constructing the solution vector **b**, the ith iteration of the solution method puts the equations of motion (46) in the form

$$\mathbf{M}(\mathbf{b}_i)\ddot{\mathbf{b}}_i + \mathbf{f}^{\sigma}(\mathbf{b}_i) = \mathbf{f}(\mathbf{b}_i) \tag{49}$$

In order to gain computational efficiency in the construction of the mass and geometric stiffness matrices, **M** and $\mathbf{k}_g$, respectively, the shape matrix, $\mathbf{N}_m$, is a reduced form of the shape matrix for the shallow shell element. The explicit form of $\mathbf{N}_m$ can be found in Ref. [15]. The validity of the present analysis is established by considering a rotating beam subjected to a spin-up maneuver [12]. In this study, the beam is modeled as a narrow plate with triangular shallow shell elements with the following boundary conditions:

$$w_0(0, y', 0) = v_0(0, y', 0) = w_0(0, y', 0) = 0$$

$$\frac{\partial w_0}{\partial x'}(0, y', 0) = \frac{\partial w_0}{\partial y'}(0, y', 0) = 0$$

The spin-up maneuver for this problem is specified as

$$\Omega(t) = \begin{cases} \Omega_0 \left[6\left(\frac{t}{T_0}\right)^5 - 15\left(\frac{t}{T_0}\right)^4 + 10\left(\frac{t}{T_0}\right)^3 \right] & t < T_0 \\ \Omega_0 & T > T_0 \end{cases}$$

where $\Omega_0 = \pi/10$ rad/sec and $T_0 = 1$ sec. The Young's and shear moduli for the beam are given as $E = 1.44 \times 10^6$ lb/ft^2 and $G = 5.54 \times 10^7$ lb/ft^2. The cross-sectional area and the length of the beam are $A = 1$ ft^2 and $L = 100$ ft, respectively. The moment of inertia about the planar axes is specified as $I = 0.08333$ ft^4. The beam has a mass density of $\rho = 5.22$ slug/ft^3. Since the beam is modeled as a plate, its thickness and width are computed as $h = 1$ ft and $W = 1$ ft based on the values given for the moment of inertia and the cross-sectional area for the beam. A comparison between the considerably large transverse and axial displacements at the tip of the plate obtained from the present analysis and those presented by Christensen and Lee is given in Fig. 3. The sequence of the motion with respect to the inertial coordinate system is depicted in Fig. 4.

The capability of the present analysis is further demonstrated by considering a laminated, cantilever blade tilted at 45° and 90° angles with respect to the (x-y) plane. The planform dimensions of the blade are specified by $L = 2.5$ m and $W = 0.2$ m. The blade thickness of $h = 0.04$ m results from a laminate lay-up of $[0°/90°_4]_s$. Each lamina has the material properties $E_L = 181$ GPa, $E_T = 10.3$ GPa, $G_{LT} = 7.17$ GPA, and $\nu_{LT} = 0.28$, with mass density $\rho = 1600$ kg/m^3. The applied spin-up maneuver is the same as that specified for the previous problem, with $\Omega_0 = 10\pi$ rad/sec and $T_0 = 0.05$ sec. The influence of tilt angle on the tip displacements is illustrated in Fig. 5. As shown in this figure, the difference in maximum tip deflections is rather significant. When the blade is tilted at a 45° angle, the difference between the transverse deflections at the left and right corners of the blade indicates that the tip of the blade undergoes twisting. These corner displacements are presented in Fig. 6. With respect to the inertial frame, the sequence of deformations for a blade tilted at angles of 0° and 45° is illustrated in Fig. 7.

Conclusions

A variational formulation that accounts for changes in motion-induced stiffness while determining the structural response of moderately thick laminated shells within the realm of a multibody dynamics formalism has been presented. This methodology also provides the inertial forces as part of the solution for corresponding external forces. Although demonstrated herein on simple geometric configurations, this analysis is general enough to treat curved laminates. This formulation represents an advancement in state-of-the-art analysis of rigid-body dynamics coupled with nonlinear elastic deformations.

References

[1] R. Bhumbla and J. B. Kosmatka, "Stability of spinning shear deformable laminated composite plates," *31st AIAA/ASME/ASCE/AHS/ASC Structures, Structural Dynamics and Materials Conference*, AIAA, New York, Part 4, pp. 1986-1993, 1990.

[2] O. A. Bauchau and W. Chiang, "Dynamic analysis of rotor flexbeams based on nonlinear anisotropic shell models," *J. Am. Helicopter Soc.* 38, pp. 55-61, 1993.

[3] J. B. Kosmatka, "An accurate shear-deformable six-node triangular plate element for laminated composite structures," *Int. J. Num. Meth. Eng.* 37, pp. 431-455, 1994.

[4] O. A. Bauchau and N. K. Kang, "A multibody formulation for helicopter structural dynamic analysis," *J. Am. Helicopter Soc.* 38, pp. 3-14, 1993.

[5] Z. E. Boutaghou, A. G. Erdman, and H. K. Stolarsi, H. K., "Dynamics of flexible beams and plates in large overall motions," ASME *J. Appl. Mech.* 59, pp. 991-999, 1992.

[6] T. Tsang, "Dynamic analysis of highly deformable bodies undergoing large rotations," Ph.D. thesis, The University of Arizona, Tucson, 1993.

[7] A. K. Banarjee and T. R. Kane, "Dynamics of a plate in large overall motion," ASME *J. Appl. Mech.* 56, pp. 887-892, 1989.

[8] A. K. Banarjee and J. M. Dickens, "Dynamics of an arbitrary flexible body in large rotation and translation," *J. Guid., Con., Dyn.* 13, pp. 221-227, 1990.

[9] B. Chang and A. A. Shabana, "Nonlinear finite element formulation for the large displacement analysis of plates," ASME *J. Appl. Mech.* 57, pp. 707-718, 1990.

[10] B. Chang and A. A. Shabana, "Total Lagrangian formulation for the large displacement analysis of rectangular plates," *Int. J. Num. Meth. Eng.* **29**, pp. 73-103, 1990.

[11] A. Tessler, "A C^0-anisoparametric three-noded shell element," *Comp. Meth. Appl. Mech. Eng.* 78, pp. 89-103, 1990.

[12] E. R. Christensen and S. W. Lee, "Nonlinear finite element modeling of the dynamics of unrestrained flexible structures," *Comp. and Struc.* 23, pp. 819-829, 1986.

[13] E. Madenci and A. Barut, "A free-formulation-based flat shell element for nonlinear analysis of thin composite structures," *Int. J. Num. Meth. Eng.* **37**, pp. 3825-3842, 1994.

[14] C. C. Rankin and F. A. Brogan, "An element independent corotational procedure for treatment of large rotations," *Trans. ASME, J. Pressure Vessel Tech.* **108**, pp. 165-174, 1986.

[15] S. Oral, "A three-node shear-flexible hybrid-stress finite element for the analysis of laminated composites plates," *J. Thermoplastic Comp. Mater.* 1, pp. 339-360, 1988.

FIGURE CAPTIONS

Figure 1. Kinematics of a point in an element due to rigid-body motion and local deformation.

Figure 2. Element coordinate system and degrees of freedom for a triangular shallow shell element.

Figure 3. Transverse and axial tip displacements along the center line of a rotating narrow plate

Figure 4. A narrow plate undergoing a sequence of deformations in reference to an inertial frame.

Figure 5. Transverse tip displacements along the center line of a rotating laminated blade.

Figure 6. Transverse tip displacements at the corners of a rotating laminated blade.

Figure 7. Sequence of deformations for a blade tilted at angles of 90° and 45°.

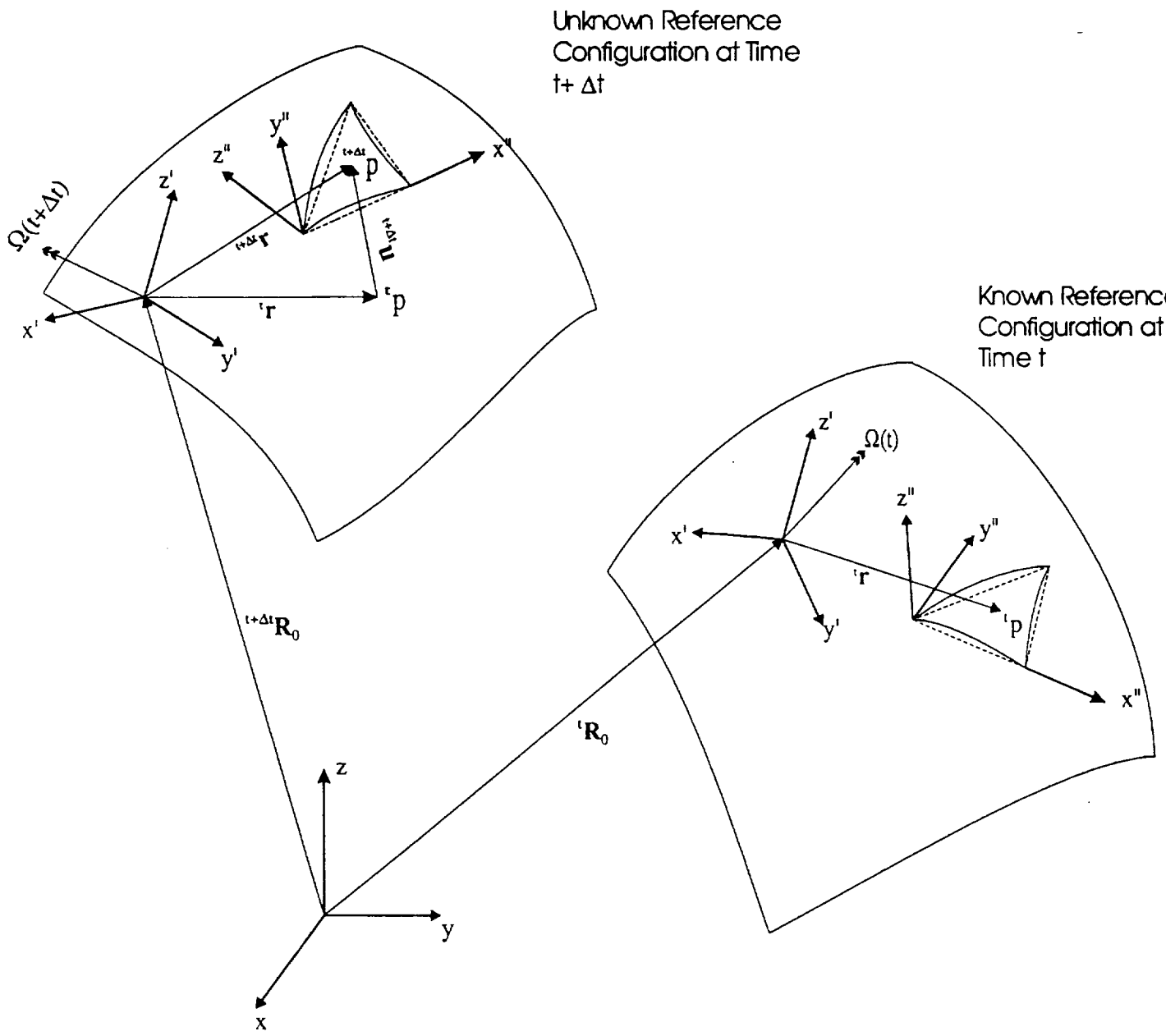
Unknown Reference
Configuration at Time
t+ Δt
Known Reference
Configuration at
Time t
Ω((t+Δt))
z'
z''
y''
x''
t+Δt p
t+Δt r
t+Δt u
x'
y'
t r
t p
t+Δt R0
t R0
Ω(t)
z
y
x

FIGURE 1

Figure 2.

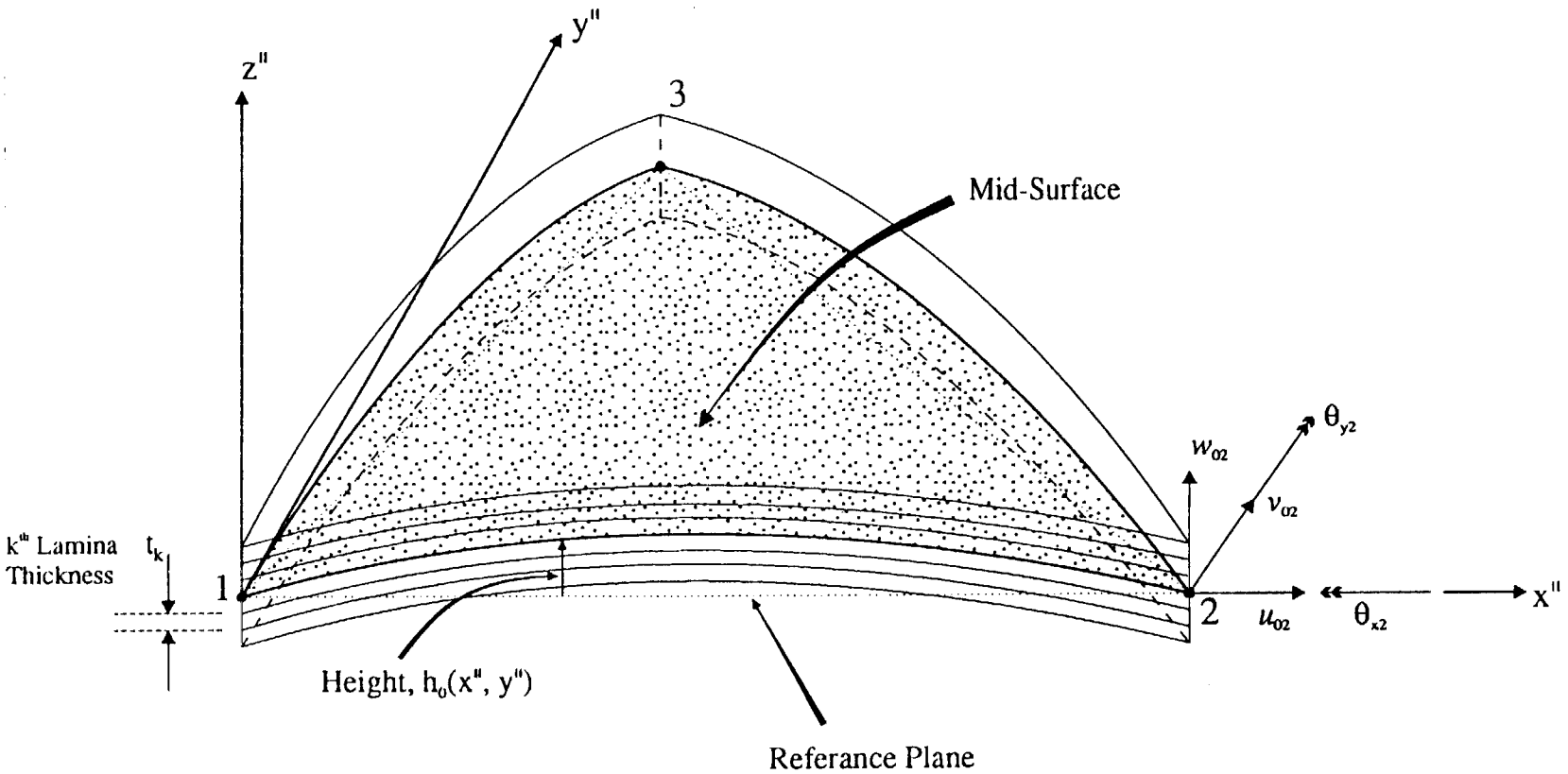
z"
y"
3
Mid-Surface
θ_{y2}
w_{02}
v_{02}
kth Lamina Thickness
t_k
1
2
u_{02}
θ_{x2}
x"
Height, $h_0(x", y")$
Referance Plane

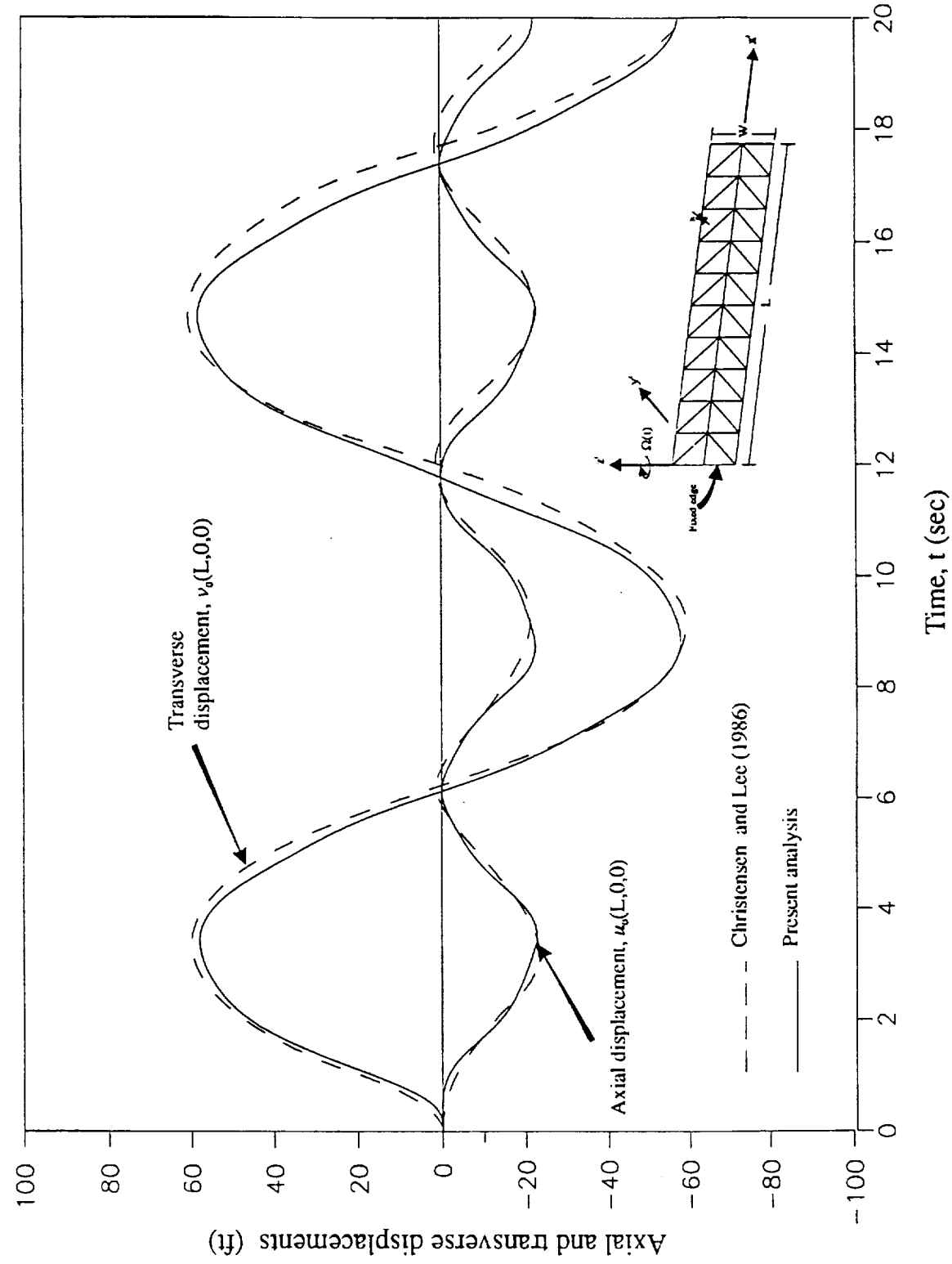
Axial and transverse displacements (ft)
100
80
60
40
20
0
-20
-40
-60
-80
-100
0
2
4
6
8
10
12
14
16
18
20
Time, t (sec)
Transverse displacement, v_0(L,0,0)
Axial displacement, u_0(L,0,0)
Christensen and Lee (1986)
Present analysis
Fixed edge
L
W

FIG. 3

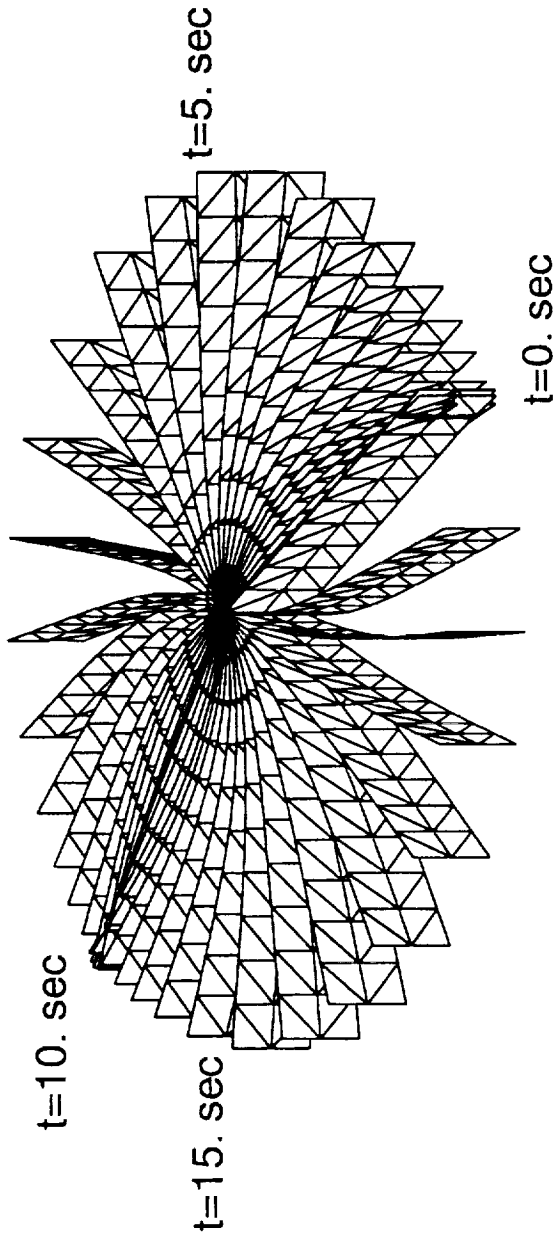

FIG. 4

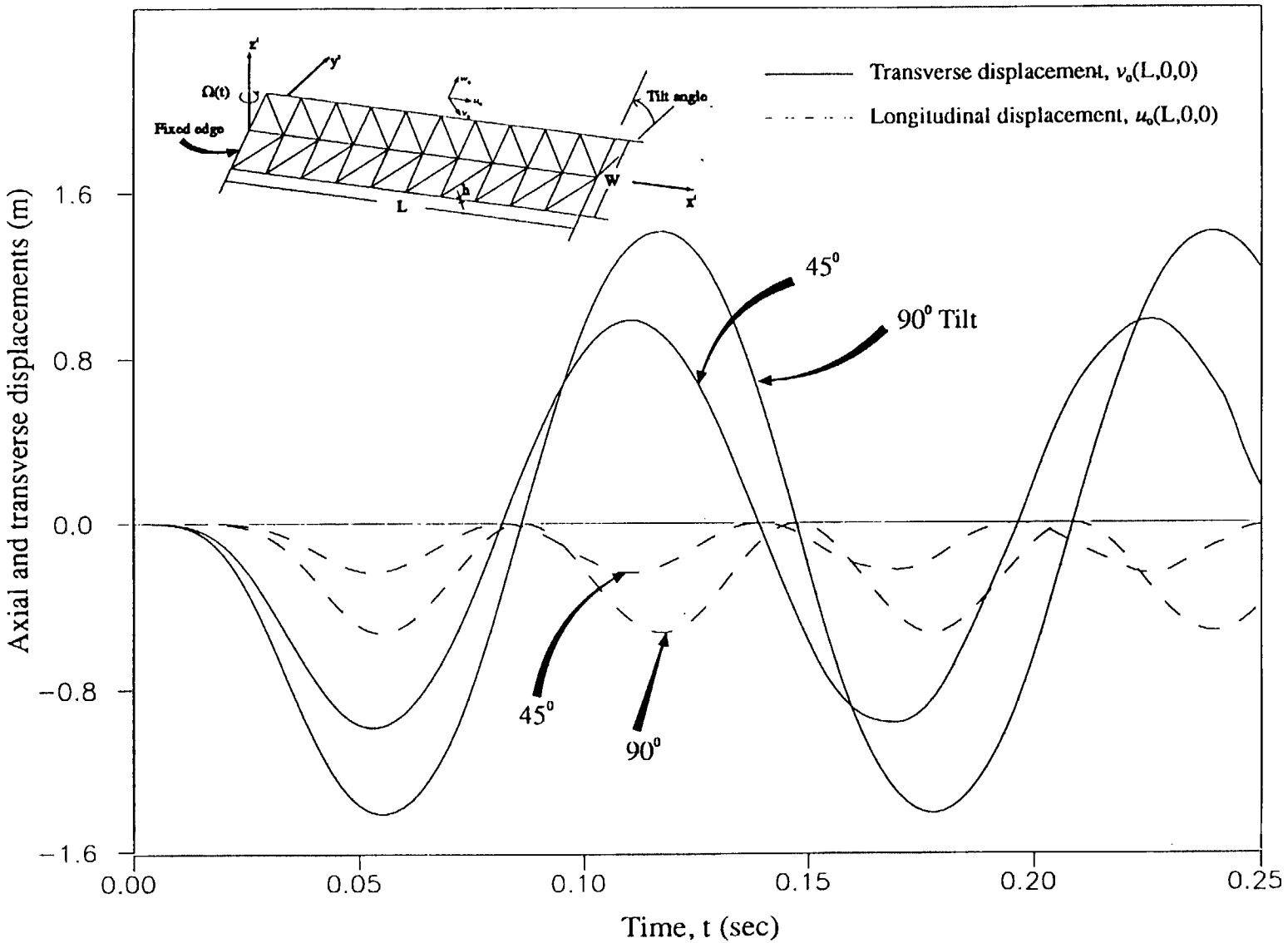
Transverse displacement, v_0(L,0,0)
Longitudinal displacement, u_0(L,0,0)
Ω(t)
Fixed edge
Tilt angle
L
W
h
45°
90° Tilt
45°
90°
Axial and transverse displacements (m)
1.6
0.8
0.0
−0.8
−1.6
0.00
0.05
0.10
0.15
0.20
0.25
Time, t (sec)

Fig. 6

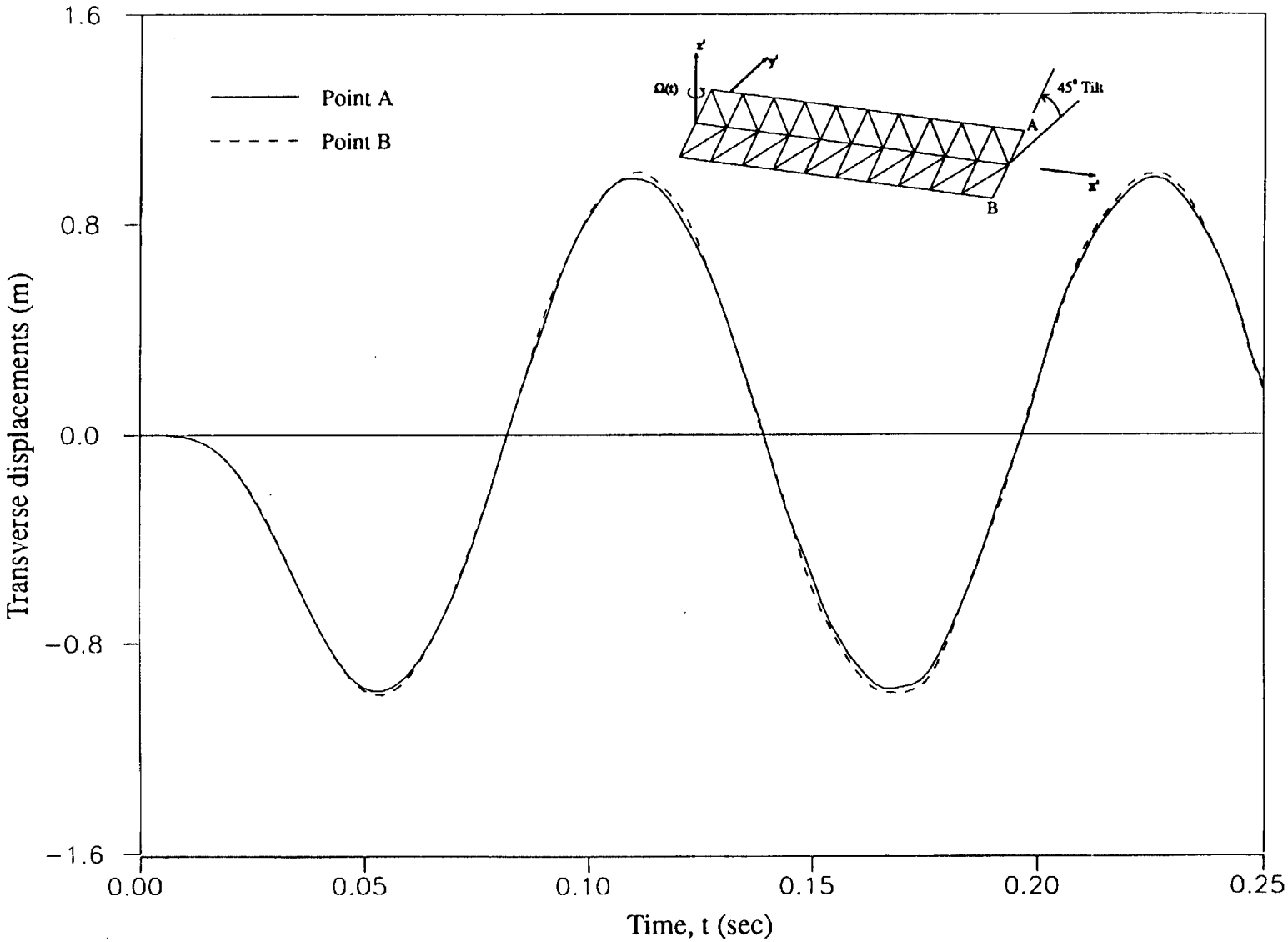
1.6
0.8
0.0
−0.8
−1.6
Transverse displacements (m)
0.00
0.05
0.10
0.15
0.20
0.25
Time, t (sec)
Point A
Point B
Ω(t)
45° Tilt
A
B

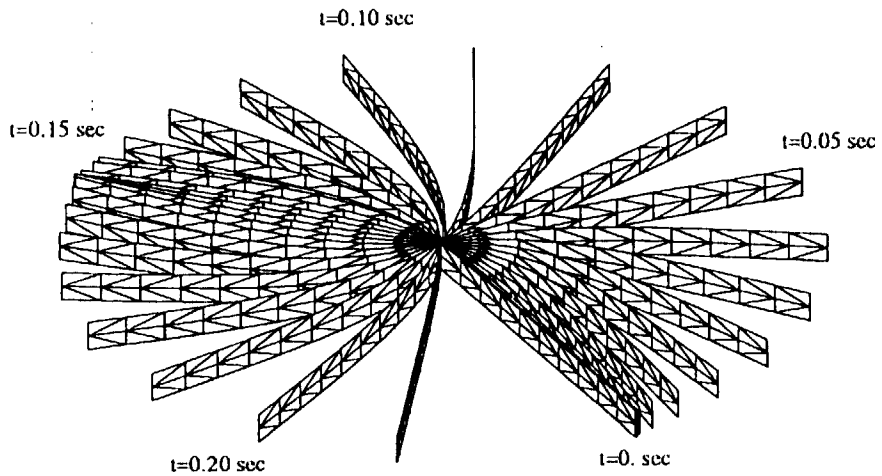

90° Tilt

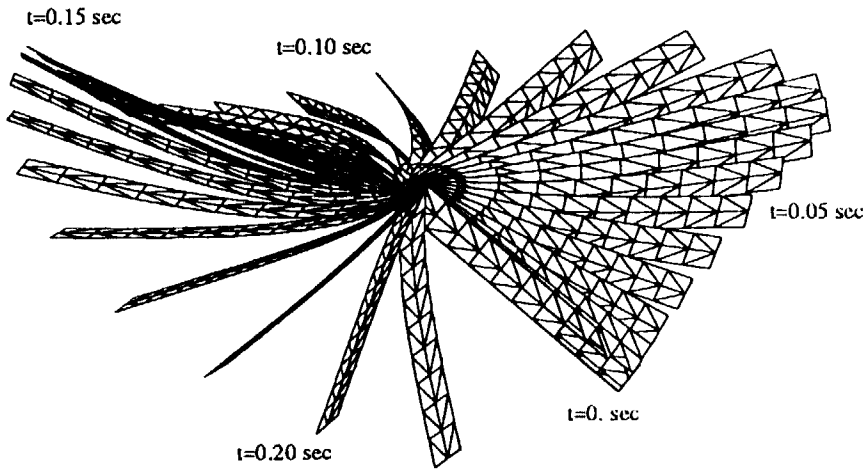

45° Tilt